Nuclear Physics **A484** (1988) 90–97
North-Holland, Amsterdam

THE FIRST EXCITED STATE IN ^{23}Al AND ITS INFLUENCE ON ^{22}Mg(p, γ)^{23}Al

M. WIESCHER and J. GÖRRES

Department of Physics, College of Science, University of Notre Dame, Notre Dame IN 46556, USA

B. SHERRILL, M. MOHAR, J.S. WINFIELD and B.A. BROWN

Physics Department, Michigan State University, East Lansing MI 48824, USA

Received 13 October 1987
(Revised 25 January 1988)

Abstract: The excitation energy of the first excited state in ^{23}Al was determined by the ^{24}Mg(^{7}Li, ^{8}He) reaction. The state is observed to be at 460 ± 60 keV and belongs to the first excited $A = 23$ isospin quartet. The results are used to compute the coefficients of the isobaric multiplet mass equation. The influence of this state, a resonance in the ^{22}Mg(p, γ) channel, on the reaction flow in rp-process nucleosynthesis is discussed in detail.

E NUCLEAR REACTIONS ^{24}Mg(^{7}Li, ^{8}He), $E = 191$ MeV; measured $\sigma(E(^{8}\text{He}))$; deduced ^{22}Mg(p, γ)^{23}Al stellar reaction rate, isobaric mass multiplet equation parameters. ^{23}Al deduced levels.

1. Introduction

The production of ^{22}Na from hot hydrogen burning in novae, supernovae or massive stars has been discussed by numerous authors [1,2]. It is thought to be produced in substantial quantities in the hot Ne-Na-cycle by:

$$^{20}\text{Ne(p, }\gamma)^{21}\text{Na(p, }\gamma)^{22}\text{Mg}(\beta^{+}\nu)^{22}\text{Na(p, }\gamma)^{23}\text{Mg}\,.$$

This reaction sequence will occur at temperature and density conditions, where the ^{21}Na(p, γ) reaction is expected to proceed more rapidly than the competing β-decay ($T_{1/2} = 22.48$ sec) [3]. At these temperatures, however, proton capture on ^{22}Mg ($T_{1/2} = 3.86$ sec), ^{22}Mg(p, γ)^{23}Al, may also occur. Due to the low Q-value of the reaction, $Q = 0.127$ MeV, at high temperatures the photodisintegration of ^{23}Al, ^{23}Al(γ, p)^{22}Mg, will prevent a substantial production of ^{23}Al after equilibrium has been reached. The abundance ratio depends on the temperature T_9 (in 10^9 K), the density ρ (g/cm^3) and the mass fraction of hydrogen X(H):

$$\frac{n(^{23}\text{Al})}{n(^{22}\text{Mg})} = 3.25 \cdot 10^{-10} T_9^{3/2} \rho X(\text{H}) \exp(1.474/T_9)$$

and is independent of the proton capture reaction rate of ^{22}Mg(p, γ)^{23}Al.

0375-9474/88/$03.50 © Elsevier Science Publishers B.V.
(North-Holland Physics Publishing Division)

However, in explosive events, triggering the rp-process [4]) in novae, accreting neutron stars and black holes [5]), the timescales involved may be too short to reach the equilibrium between proton capture on ^{22}Mg and photodisintegration of ^{23}Al. The production or depletion of ^{22}Mg depends largely on the original abundances $[N_i]$, the capture rates $\lambda_{i,1}$, and the rates for the β-decay $\lambda_{i\beta}$ and the photodisintegration $\lambda_{i\gamma}$:

$$\frac{\mathrm{d}}{\mathrm{d}t}[^{22}\mathrm{Mg}] = -\lambda_{22,1}[^{22}\mathrm{Mg}][\mathrm{H}] - \lambda_{22\beta}[^{22}\mathrm{Mg}] + \lambda_{21,1}[^{21}\mathrm{Na}][\mathrm{H}] + \lambda_{23,\gamma}[^{23}\mathrm{Al}] .$$

The current proton capture rates for ^{21}Na(p, γ)^{22}Mg and ^{22}Mg(p, γ)^{23}Al are estimated mainly on the basis of nuclear structure information of the particular compound nuclei [3,6]).

However, the rate of ^{22}Mg(p, γ)^{23}Al is still very uncertain [6]). Due to the low proton threshold Q, the reaction rate will be determined by the nonresonant f-wave direct capture to the ground state and by the s-wave resonant capture to the first excited state in ^{23}Al. The resonant part of the rate depends exponentially on the resonance energy and linearly on its resonance strength $\omega\gamma$, neither of which is known. The mirror level in ^{23}Ne has an excitation energy of 1.02 MeV [ref. [7])], its pronounced single-particle structure suggests a large Thomas–Ehrman shift between the mirror states. This indicates that the resonance in ^{22}Mg(p, γ)^{23}Al may contribute at significantly lower energies than suggested before [4,6]).

In the present work we will describe an experiment to determine the excitation energy of the first excited state in ^{23}Al and will discuss its implications for the reaction rate of ^{22}Mg(p, γ)^{23}Al.

2. Experimental procedure and analysis

We measured the reaction ^{24}Mg(^{7}Li, ^{8}He)^{23}Al to determine the level energy of the first excited state in ^{23}Al. The experiment was performed at the NSCL Cyclotron Laboratory at MSU. An enriched ^{24}Mg target (6.25 mg/cm^2) was bombarded with a 191 MeV ^{7}Li beam from the K500 cyclotron. The reaction particles were detected in the focal plane of the S-320 spectrometer [8]) by a detector system consisting of two single-wire proportional counters and two ionization chambers, backed by a plastic scintillator. These served for very clean particle identification by $E \times \Delta E$ and time-of-flight methods. Due to the target thickness (330 keV) and the energy resolution of the spectrometer ($\approx$200 keV), the expected FWHM-energy resolution was limited to $\approx$390 keV. To monitor energy shifts of the ^{7}Li beam and to maintain energy calibration of the ^{8}He spectrum, calibration measurements on ^{9}Be(^{7}Li, ^{8}He) and ^{40}Ca(^{7}Li, ^{8}He) were done regularly. No shifts, other than a slow drift in the dipole field, were observed over the approximately 5 day run. All spectra were shifted to correct for the $\approx$1G dipole drift, measured with an NMR probe.

Fig. 1 shows the spectrum obtained from the ^{24}Mg(^{7}Li, ^{8}He)^{23}Al reaction. The spectrum is a composite of 9 runs on Mg targets, at $\theta = 5°$, with a total accumulated charge of 1.2 mCb. The peak shape and the resolution was determined from the well-resolved ground-state transitions in the calibration reactions ^{9}Be and ^{40}Ca(^{7}Li, ^{8}He). The focal plane of the spectrometer was calibrated by observing the peak positions of the ground-state transition and the transition to the first excited state (0.78 MeV) in ^{9}Be(^{7}Li, ^{8}He)^{8}B along with the position of the ^{23}Al ground state, at the same magnetic field settings. The beam energy was determined from the difference in focal plane position between the ^{9}Be(^{7}Li, ^{8}He)^{8}B(gs) reaction and ^{58}Ni(^{7}Li, ^{7}Li^{+2}) elastic scattering. The calibration was checked by measuring the excitation spectra from (^{7}Li, ^{6}He) reactions on targets of ^{9}Be, ^{24}Mg and ^{58}Ni. From the comparison we estimate the calibration uncertainty to be less than 10 keV.

The ground state in ^{23}Al, $J^{\pi} = \frac{5}{2}^{+}$, is strongly populated, $\sigma = 0.7(4)$ μb/sr; the spectrum also indicates strong transitions to unresolved levels between 2.5 and 3.7 MeV excitation energy (see the broad, unresolved peak structure between channel 570 and channel 600 of the spectrum (1 k) shown in fig. 1). The transition to the first excited state in ^{23}Al, $J^{\pi} = \frac{1}{2}^{+}$, could be identified as a pronounced shoulder,

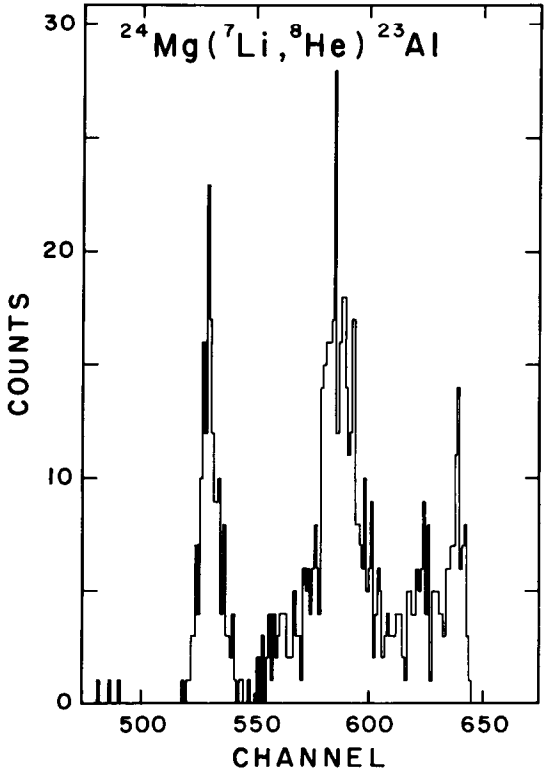

Fig. 1. Spectrum (1k) of the ^{24}Mg(^{7}Li, ^{8}He)^{23}Al reaction measured at $\theta = 5°$.

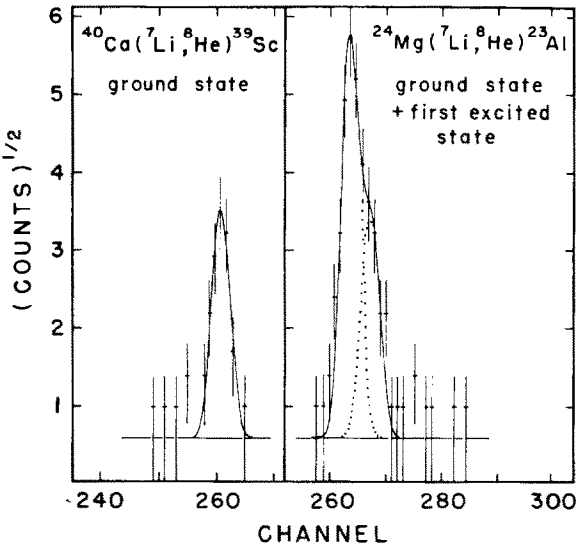

Fig. 2. Analysis of the transitions to the ground state and the first excited state in ^{23}Al as described in the text. For a better presentation the data of fig. 1 are compressed by a factor two and shown as a square root plot. Peak shape parameters were obtained from the ground-state transition in ^{40}Ca(^{7}Li, ^{8}He)^{39}Sc, shown on the left-hand side.

$\sigma = 0.2(1)$ μb/sr, on the low-energy side of the ground-state peak. Fig. 2 (right-hand side) exhibits this part of the data from fig. 1 as a compressed square root plot (0.5 k). Also shown, on the left-hand side of the figure, is the ground-state transition in ^{40}Ca(^{7}Li, ^{8}He)^{39}Sc measured at identical experimental conditions. Its fit gives the peak shape and the peak width of 420 keV, mainly determined by the spectrometer resolution and the target thickness. The so-obtained experimental peak width was applied in fitting the ^{24}Mg(^{7}Li, ^{8}He) transition to the ground state and the first excited state of ^{23}Al. The fit to these two transitions is shown in fig. 2 and yields an excitation energy of $E_x = 460 \pm 60$ keV for the first excited state in ^{23}Al. This result also agrees with a previous study of ^{23}Al by ^{28}Si(^{3}He, ^{8}Li)^{23}Al at bombarding energies of 76.3 MeV [ref. [9])]. The measured spectrum (resolution 150 keV) indicates a weak peak, shown in fig. 2 of ref. [9]), but not assigned by those authors. In the light of the present data, this peak can be assigned to the transition to the first excited state in ^{23}Al. Reanalysis yields an excitation energy of $E_x = 475 \pm 50$ keV, well in agreement with the present results.

3. Results and discussion

The isobaric multiplet mass equation (IMME) relates the masses of the $2T+1$ members of a multiplet with isobaric spin T and is given by [10]):

$$M(T_z) = a + bT_z + cT_z^2,$$

where T_z is the z-component of the isospin $T_z = 0.5(N-Z)$ and a, b, c the IMME coefficients. In principle, this equation relates the masses of any multiplet of analog levels.

The measurement of the excitation energy of the first excited state in ^{23}Al, $J^\pi = \frac{1}{2}^+$, $T = \frac{3}{2}$, in combination with the known excitation energies of the $T = \frac{3}{2}$ analog states in ^{23}Na and ^{23}Ne [ref. [7])], allows the computation of the IMME coefficients for the first excited $A = 23$ isospin quartet. Table 1 shows the derived parameter in comparison with the IMME coefficients for the $T = \frac{3}{2}$ ground-state quartet [10]). Also included in table 1 are the $A = 23$ $J^\pi = \frac{5}{2}^+, \frac{1}{2}^+$ b and c coefficients obtained with the recent empirical isospin-nonconserving (INC) interaction of Ormand and Brown [11]). The ground state ($J^\pi = \frac{5}{2}^+$) experimental values agree reasonably well with those calculated; however the b and c coefficients obtained from the excited state ($J^\pi = \frac{1}{2}^+$) are not in good agreement. As explained by Ormand and Brown for the similar case of $A = 17$, since the Ormand-Brown interaction is based on harmonic-oscillator wave functions this deviation is most likely a result of the small binding energy of the $1s_{1/2}$ proton states, which results in a large rms charge radius and a smaller Coulomb energy.

TABLE 1

Coefficients of the isobaric-multiplet mass equation (in MeV) for the ground state and first excited state $A = 23$ isobaric quartet

A	J^π	b	c	Ref.
23	$\frac{5}{2}^+$	-3.973 ± 0.008	0.230 ± 0.004	[10])
		-3.924	0.255	INC [11])
23	$\frac{1}{2}^+$	-3.789 ± 0.022	0.259 ± 0.010	present
		-3.913	0.221	INC [11])

4. Astrophysical implications

The weighted average of the present result and that of Benenson *et al.* [9]) yields an excitation energy of $E_x = 470 \pm 40$ keV, which corresponds to a resonance energy in ^{22}Mg(p, γ)^{23}Al of $E_r^{lab} = 360 \pm 40$ keV. This is significantly lower than previously suggested [6]).

The resonance strength is determined by the partial widths Γ_p, Γ_γ and the total width $\Gamma_{tot} = \Gamma_p + \Gamma_\gamma$ of the level:

$$\omega\gamma = \frac{\Gamma_p \Gamma_\gamma}{\Gamma_{tot}}.$$

The proton width can be derived from the single-particle spectroscopic factor C^2S

of the state by:

$$\Gamma_p = 3\frac{\hbar^2}{\mu R^2} C^2 S P_l$$

where P_l is the Coulomb penetrability evaluated at the nuclear radius R, and μ is the reduced mass. The gamma width can be computed from the reduced E2 transition probability B(E2) for the γ-decay of the level ($\frac{1}{2}^+$) to the ground state ($\frac{5}{2}^+$). Shell-model calculations, using the Brown-Wildenthal universal sd-model [12]), yield for the spectroscopic factors of the ground and the first excited state $C^2S_0 = 0.34$ and $C^2S_1 = 0.66$, respectively. The results agree well with the known values for the mirror states in ^{23}Ne, $C^2S_0 = 0.22$, $C^2S_1 = 0.7$ [ref. [7])]. Using the same code, the reduced transition probability was calculated as $B(\mathrm{E2}) = 20.4\, e^2\,\mathrm{fm}^4$. The resulting partial widths, $\Gamma_p = 32^{+53}_{-23}$ eV and $\Gamma_\gamma = 2.5^{+1.2}_{-0.9} \cdot 10^{-7}$ eV, allows the determination of the resonance strength

$$\omega\gamma = 2.5^{+1.2}_{-0.9} \cdot 10^{-7}\ \mathrm{eV}\,.$$

Following Fowler *et al.* [13]), the resonant reaction rate can be derived from:

$$N_A\langle\sigma v\rangle_{\mathrm{res}} = 1.65 \cdot 10^5 T_9^{-3/2} \omega\gamma \exp\left(-11.605 E_r^{\mathrm{c.m.}}/T_9\right) \qquad \mathrm{cm^3\ mole^{-1}\ s^{-1}}\,,$$

where T_9 is the burning temperature in 10^9K, $E_r^{\mathrm{c.m.}}$ is the center-of-mass resonance energy in units of MeV and $\omega\gamma$ the resonance strength in units of eV. The resulting reaction rate is shown in fig. 3.

The nonresonant part of the reaction rate is dominated by the f→d E1-direct capture transition to the ground state in ^{23}Al. Possible d→d M1, E2- and s→d E2-transition contributions are negligible; 4% and 1% with respect to the E1-transition strength. The cross section for the process depends linearly on the spectroscopic factor of the final state [14]). Wiescher *et al.* [6]) used in their previous estimate of the direct capture a slightly smaller spectroscopic factor than suggested by the shell-model calculations. This will increase the nonresonant rate to:

$$N_A\langle\sigma v\rangle_{\mathrm{dc}} = 3.66 \cdot 10^6 T_9^{-2/3} \exp\left(-21.94 T_9^{-1/3}\right) \qquad \mathrm{cm^3\ mole^{-1}\ s^{-1}}\,.$$

In fig. 4 we compare the present results with previous suggestions for the rate of ^{22}Mg(p, γ)^{23}Al [refs. [4,6])]. The large discrepancies with ref. [4]) at low temperatures results from the neglect of the direct capture and are discussed in ref. [6]). Compared to the rate of [6]) the new rate shows a slight enhancement at temperatures $0.1 \leq T_9 \leq 1.0$, due to the significantly lower resonance energy.

The reaction rate contributions are shown in fig. 3. The shaded area indicates the lower and upper limit for the resonance rate caused by the uncertainties in resonance energy and resonance strength. In the temperature range $T_9 = 0.1$ to 1.0, the resonant part clearly dominates the rate, while at higher temperatures, the direct capture is more influential due to the lack of high-energy resonances.

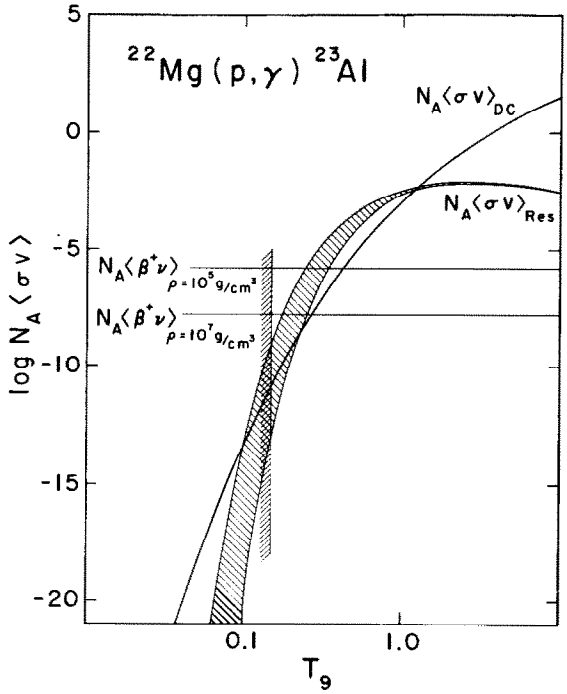

Fig. 3. Shown is the resonant and nonresonant reaction rate of ^{22}Mg(p, γ)^{23}Al. The shaded area in the resonant contribution indicates the uncertainty due to the uncertainty of the level energy. The shaded bar at $T_9 \approx 0.15$ marks the temperature range where ^{22}Mg will be produced by ^{21}Na(p, γ)^{22}Mg [3]). Also shown for comparison are the β-decay rates of ^{22}Mg (in units cm^3 mole^{-1} sec^{-1}) for two different densities, where the decay rate scales linearly with the density.

The shaded line marks the stellar temperature above which ^{22}Mg will be produced in significant amounts by the reaction ^{21}Na(p, γ)^{22}Mg [ref. [3])]. Also indicated is the β-decay rate (in units cm^3 mole^{-1} s^{-1}) of ^{22}Mg for two different densities $\rho = 10^5$ and 10^7 g/cm^3, which are typically assumed in explosive environments. This suggests that at nova conditions, $T_9 \leq 0.5$, $\rho = 10^3$-10^5 g/cm^3, no break out via the (p, γ) reaction will occur and the material, processed by ^{21}Na(p, γ)^{22}Mg (for $T_9 > 0.2$ [ref. [3])]), will decay to ^{22}Na. On accreting neutron stars, at high temperatures beyond $T_9 = 0.4$ and densities $\rho > 10^6$ g/cm^3 [ref. [5])], the (p, γ) rate exceeds sufficiently the competing β-decay rate; in the short timescales of the thermal runaway, before equilibrium with the inverse photodisintegration will take place, significant amounts of ^{22}Mg will be processed towards higher mass isotopes. More detailed reaction network calculations are necessary to analyse quantitatively the reaction flow at different temperature and density conditions.

We thank the NSCL operating staff for the excellent beam conditions. We also would like to thank E. Adimedes, W. Benenson and J. Clayton for the help during

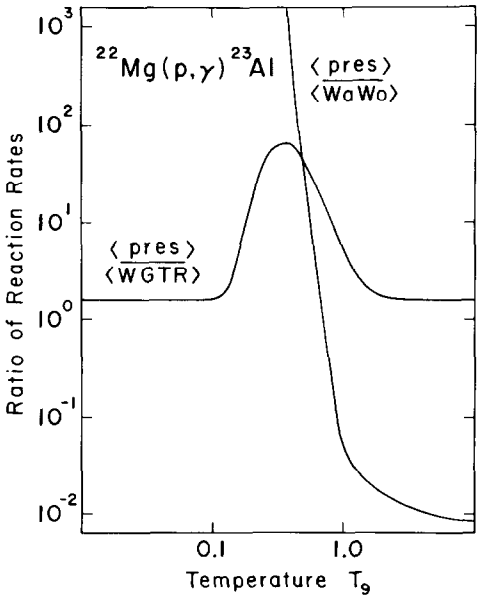

Fig. 4. The present total reaction rate of ^{22}Mg(p, γ)^{23}Al in comparison with previous estimates [4,6]).

the experiment and for helpful comments and discussions on various subjects discussed in this paper. This work was supported by the NSF grants PHY 86-11210 and PHY 84-21302.

References

1) D.D. Clayton and F. Hoyle, Ap. J. Lett. **187** (1974) L101
2) W. Hillebrandt and F.K. Thielemann, Ap. J. **255** (1982) 617
3) M. Wiescher and K. Langanke, Z. Phys. **A325** (1986) 305
4) R.K. Wallace and S.E. Woosley, Ap. J. Suppl. **45** (1981) 389
5) R.E. Taam, Ann. Rev. Nucl. Part. Sci. **35** (1985) 1
6) M. Wiescher, J. Görres, F.K. Thielemann and H. Ritter, Astron. Astrophys. **160** (1986) 56
7) P.M. Endt and C. van der Leun, Nucl. Phys. **A310** (1978) 1
8) B. Sherrill, PhD thesis, Hadr. J. Suppl., to be published
9) W. Benenson, A. Guichard, E. Kashy, D. Mueller, H. Nann and L.W. Robinson, Phys. Lett. **B58** (1975) 46
10) W. Benenson and E. Kashy, Rev. Mod. Phys. **51** (1979) 527
11) W.E. Ormand and B.A. Brown, Nucl. Phys. A to be submitted
12) B.A. Brown and B.H. Wildenthal, Nucl. Data. Tabl. **33** (1985) 347
13) W.A. Fowler, G.R. Caughlan and B.A. Zimmerman, Ann. Rev. Astr. Ap. **13** (1975) 69
14) C. Rolfs, Nucl. Phys. **A217** (1973) 29